ACADEMIA ROMÂNĂ
Revue Roumaine de Chimie
http://web.icf.ro/rrch/

Rev. Roum. Chim.,
2014, *59*(3-4), 235-243

THERMAL BEHAVIOR AND DECOMPOSITION OF MIXED VALENCE SOLIDS In_5Ch_5Cl (Ch = S, Se)

Kledi XHAXHIU,[a,*] Teodor KOTA,[b] Arjan XHELAJ[b] and Hans-Jörg DEISEROTH[c]

[a] Department of Chemistry, Faculty of Natural Sciences, University of Tirana, Blv. Zog I, 1001, Tirana, Albania
[b] Department of Physics, Faculty of Natural Sciences, University of Tirana, Blv. Zog I, 1001, Tirana, Albania
[c] Institute of Inorganic Chemistry, University of Siegen, Adolf-Reichwein-Str. 2, 57076 Siegen, Germany

Received September 23, 2013

The thermal behavior of mixed valence crystalline In_5Ch_5Cl (Ch = S, Se) is studied by high temperature powder XRD and DTA measurements. Both isostructural compounds, In_5S_5Cl and In_5Se_5Cl crystallize in the monoclinic primitive cell and space group $P2_1/m$. The high temperature XRD powder patterns recorded within 296-873 K for In_5S_5Cl exhibit a linear variation of lattice constant *c* characterized by a thermal expansion coefficient of $\alpha = 1.4(3) \times 10^{-5}$ K^{-1} and non linear behavior for the lattices *a* and *b* with respective expansion coefficients of $\alpha = 1.66(4) \times 10^{-5}$ K^{-1} and $1.31(3) \times 10^{-5}$ K^{-1}. Unlike In_5S_5Cl, the compound In_5Se_5Cl exhibits linear elongations along *a* and *b* directions with $\alpha_a = 1.5(3) \times 10^{-5}$ K^{-1}, $\alpha_b = 1.2(2) \times 10^{-5}$ K^{-1} and a nonlinear expansion along *c* direction, with a mean coefficient of $\alpha = 5.4(3) \times 10^{-6}$ K^{-1}. The DTA of both samples reveal incongruent melting. At 873 K, the powder patterns confirm the full decomposition to In_2S_3 and In_2Se_3 and other binary compounds. By the combination of these techniques a decomposition mechanism is proposed for each of them.

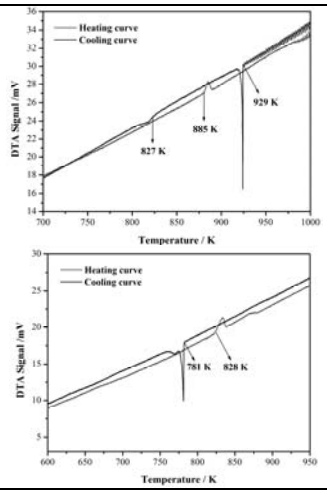

INTRODUCTION

The compounds In_5Ch_5Cl (Ch = S, Se) represent interesting mixed valence systems containing indium simultaneously three different oxidation states.[1-3] These systems inherit the concept of characteristic and common building motifs observed in most of the existing mixed valence compounds of indium.[4-10] Along with it, they bear several mikro- and nanoscopic structural anomalies[1-3] related with their real structure. In_5S_5Cl and In_5Se_5Cl are *n*-type semiconductors with single crystal resistivities of up to 1 TΩ.[11] Their needle-shaped morphology interlaced with numerous structural characteristics, display in them appealing photoelectric properties[11] for different industrial applications.

Powder diffractometry is widely used as a non-destructive analytical method for characterization of crystalline materials. The basics of the method are described by Bragg's law $2d\sin\theta = n\lambda$. This equation correlates the known Bragg angle θ, and the wavelength λ (Cu-radiation) with the unknown lattice spacing d. Because of precise adjustment and randomly oriented powder particles in capillaries the Debye-Scherrer technique provides reliable intensities from only a small amount of substance. The combination of this powerful tool with controlled temperature variation makes possible the in-situ investigation of different crystalline solid structures. Taking advantage of this fact, we aim to investigate herein the thermal behaviour of these unusual ternary mixed valence compounds and to elucidate the mechanism of their thermal decomposition.

* Corresponding author: kledi.xhaxhiu@fshn.edu.al; Cel. +355672547800

RESULTS AND DISCUSSION

1. Lattice thermal expansion of In_5Ch_5Cl (Ch = S, Se)

Sequent powder diffraction measurement at increasing temperatures in 2θ range of 5-60° are displayed in Fig. 1. To follow the cell expansion in each case a dashed line is drawn. The increase of cell dimensions increases the lattice plane distances shifting therefore the reflections toward smaller 2θ angles.

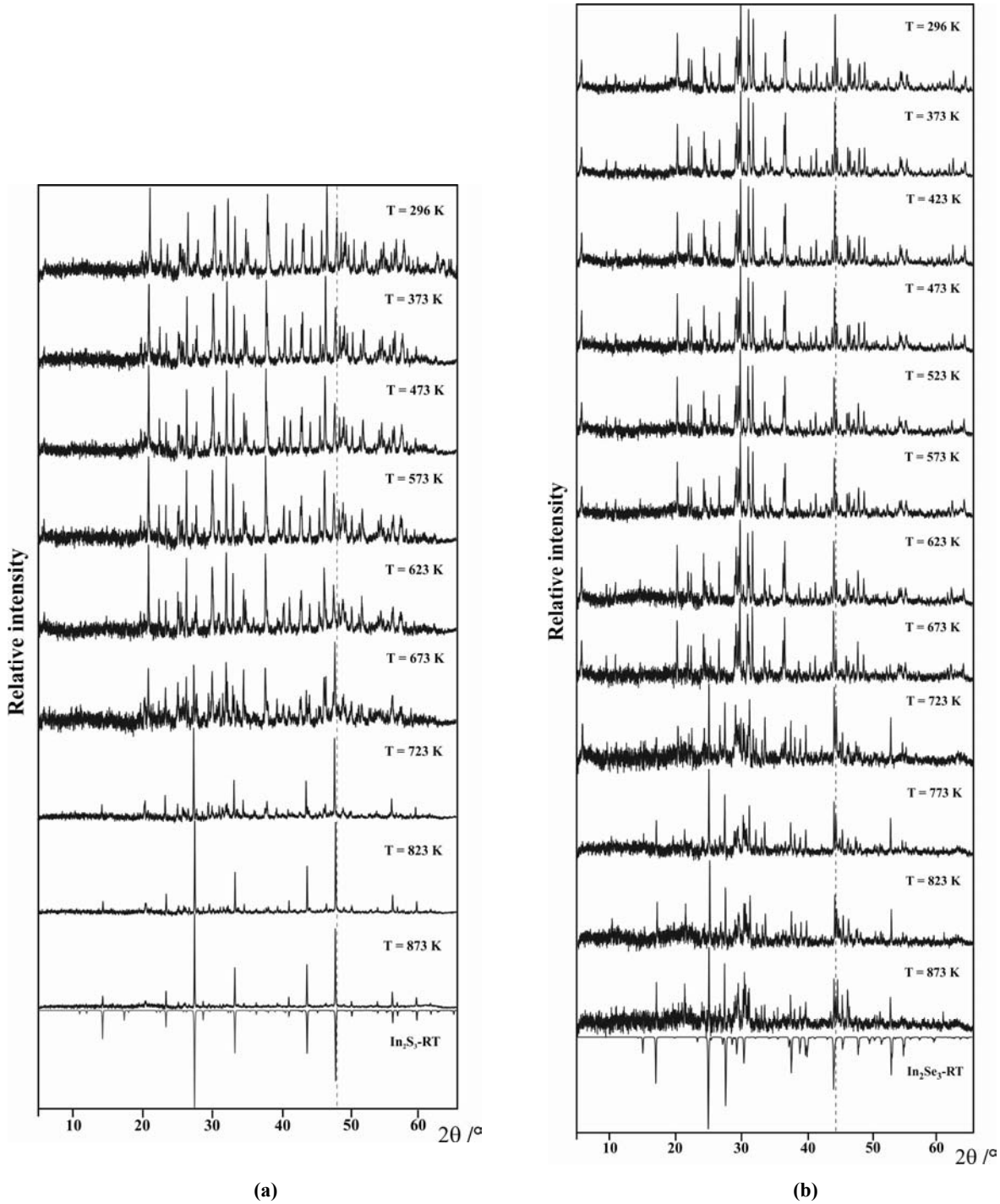

Fig. 1 – Powder diffraction patterns of: a) In_5S_5Cl, b) In_5Se_5Cl measured at different temperatures. The dashed line in each case exhibits the displacement of the chosen reflection to lower 2θ - values with temperature increase. The reversed powder pattern at the bottom of each row corresponds to the calculated diffraction patterns of In_2S_3/In_2Se_3.

All powder pattern lines measured at room temperature for both compounds could be indexed in the monoclinic primitive cell with the space group $P2_1/m$. The consequent diffraction patterns obtained at selected temperatures are given in Fig. 1. The thermal variation of their lattice parameters as a function of temperature for the considered temperatures is plotted in Fig. 2.

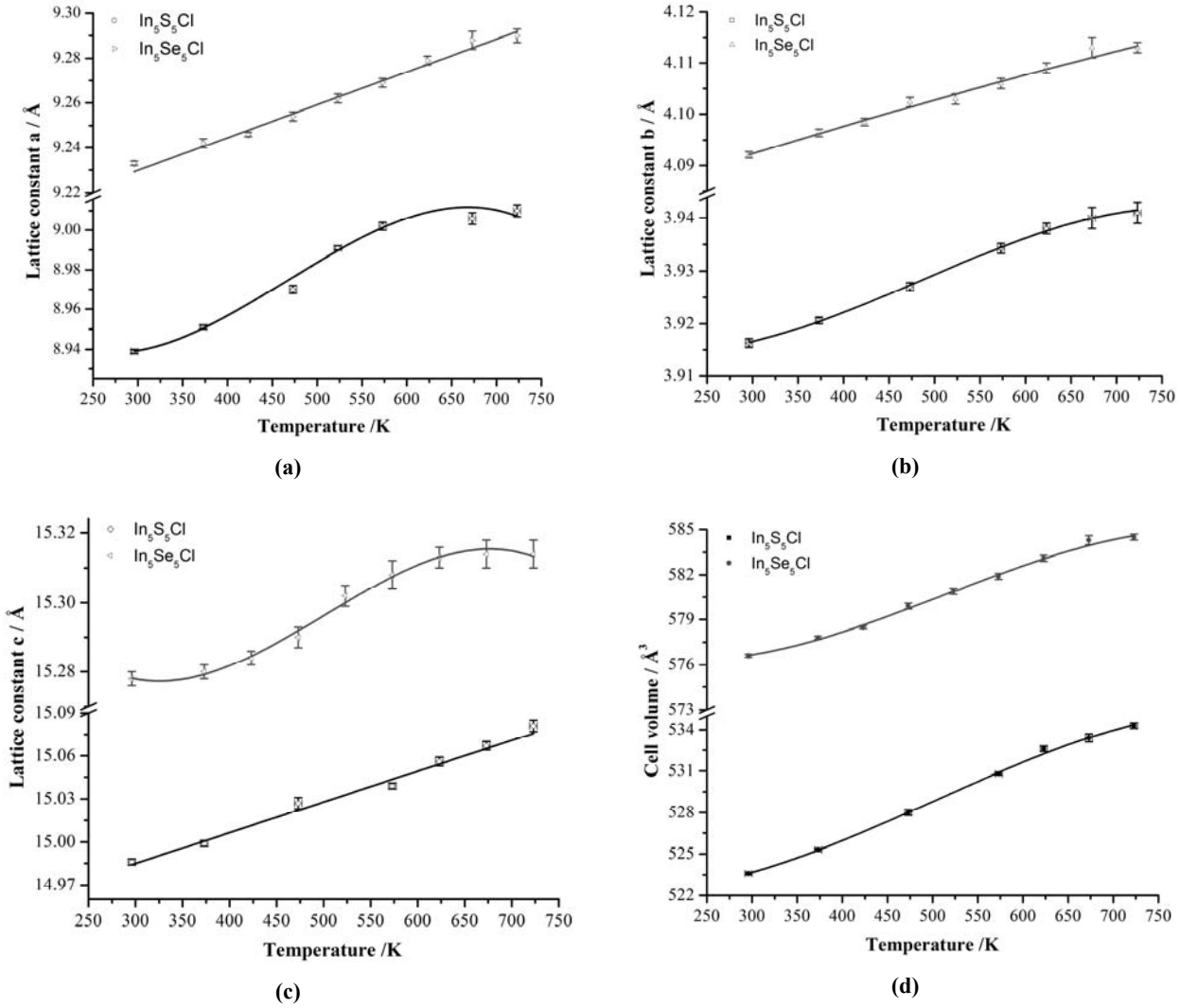

Fig. 2 – Temperature dependence of the lattice parameters: (a) a, (b) b, (c) c and (d) volume of In_5S_5Cl and In_5Se_5Cl.

Table 1

Polynomial equations fitted to the experimental points
of the lattice parameters at different temperatures for In_5S_5Cl, In_5Se_5Cl

In_5S_5Cl	$\mathbf{a(T),\ b(T) = P_1 + P_2(T\text{-}T_0) + P_3(T\text{-}T_0)^2 + P_4(T\text{-}T_0)^3}$	**(3)**
	$\mathbf{c(T),\ V(T) = P_1 + P_2(T\text{-}T_0)}$	**(4)**
In_5Se_5Cl	$\mathbf{a(T),\ b(T),\ V(T) = P_1 + P_2(T\text{-}T_0)}$	**(5)**
	$\mathbf{c(T) = P_1 + P_2(T\text{-}T_0) + P_3(T\text{-}T_0)^2 + P_4(T\text{-}T_0)^3}$	**(6)**

Table 2

Fitting parameters for the equations 3-6 of Table 1

In_5S_5Cl	P_1	P_2	P_3	P_4	χ^2	R^2
a	8.9391(7)	$1.2(2) \times 10^{-4}$	$5(1) \times 10^{-7}$	$-9(1) \times 10^{-10}$	0.48434	0.99937
b	3.9164(8)	$4.0(8) \times 10^{-5}$	$1.8(5) \times 10^{-7}$	$-3.1(8) \times 10^{-10}$	0.19995	0.99894
c	14.984(2)	$2.10(9) \times 10^{-4}$	-	-	2.14819	0.9902
V	523.5 (1)	$2.63(6) \times 10^{-2}$			3.41683	0.99676
In_5Se_5Cl	P_1	P_2	P_3	P_4	χ^2	R^2
a	9.231(1)	$1.4(6) \times 10^{-4}$	-	-	2.06725	0.98443
b	4.0923(3)	$5.0(2) \times 10^{-5}$			0.57631	0.99262
c	15.278(1)	$-6(2) \times 10^{-5}$	$1.1(1) \times 10^{-6}$	$-1.8(2) \times 10^{-9}$	0.25097	0.99469
V	576.54 (1)	$1.95(8) \times 10^{-2}$			3.77768	0.98964

The temperature dependence of lattice parameters for both considered compounds is expressed by the polynomial equations (3), (4) and (5), (6) listed in Table 1. The corresponding fitting parameters obtained by the least-squares fittings using Marquardt algorithm and are listed in Table 2.

Despite of the isotypic character of the structures of In_5S_5Cl and In_5Se_5Cl the temperature dependence of their lattice constants displayed in Fig. 2 shows significant changes. The temperature variation of the lattice constants **a** and **b** for In_5S_5Cl obeys to a third order function, unlike the lattice constant **c** and the unit cell **volume** which exhibit a linear variation. In contrast to it, the lattice constants **a, b** and the unit cell **volume** of In_5Se_5Cl vary linearly from temperature; meanwhile, the lattice constant ***c*** obeys to a third order function (s-shaped) from temperature. Thermal expansion coefficients were calculated according to the equations (7) and (8). The found values for the lattice constants **a** and **b** of In_5S_5Cl and for the lattice constant ***c*** of In_5Se_5Cl which deviate from linearity are listed in Fig. 4. The thermal behavior of both investigated compound shows no phase transition within the studied temperature range.

2. Structure & structural characteristics of In_5Ch_5Cl (Ch = S, Se)

The compounds In_5Ch_5Cl (Ch = S, Se) are isotypic and crystallize in the monoclinic crystal system with the space group $P2_1/m$. [1-3] Based on the nomenclature proposed by Robin,[12] these compounds belong to the first group of mixed valence compounds where, indium occurs simultaneously in three different oxidation states: In^+, formal In^{2+} and In^{3+}. Meanwhile the sulfur/selenium and chlorine atoms possess their lowest oxidation numbers [Ch^{2-}] and [Cl^-]. The explicit formula of these compounds can be written as follows: In_5Ch_5Cl = [In^+] [$(In_2)^{4+}$] 2[In^{3+}] 5[Ch^{2-}] [Cl^-] (Ch = S, Se). For better visualization of the structure, the direction along [010] is considered (Fig. 3). The three different indium species exhibit characteristic local coordinations. In^+ is located in three capped trigonal prismatic holes (Fig. 3c); In^{2+} builds with its neighbored In^{2+} covalent bonded dumbbells $(In_2)^{4+}$, where each indium atom is further coordinated by three chalcogenides (Fig. 3c), meanwhile In^{3+} is octahedrally coordinated (Fig. 3c). Similar to existing mixed valence binary and ternary indium chalcogenides,[4-10] this structure is built up by two different repeating building units regarded as two dimensional motives. One motif is characteristic for this kind of structure and the other one is common for other structures too (Fig. 3b). The characteristic motif is built up from cis- and trans edge-sharing $InCh_4Cl_2$/$InCh_4Cl_2$ octahedra double-chains which share edges and corners with the three capped trigonal prismatic units occupied by In^+ species (Fig. 3b top). The common motif is similar to the existing mixed valence binary and ternary indium chalcogenides, and is built up of cis and trans edge-sharing octahedra double-chains bonded to chains of ethane analogues In_2Ch_6 fragments (Fig. 3b bottom).

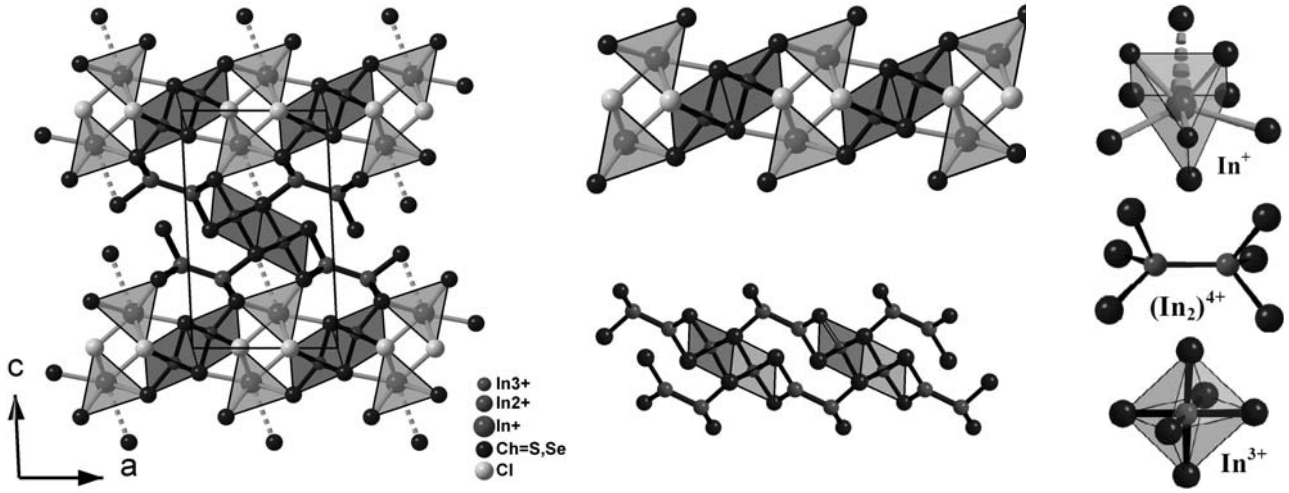

Fig. 3 – (a) Projection of the structure of In_5Ch_5Cl (Ch = S, Se) along [010], (b-top) characteristic building motif made up of cis and trans edge-sharing $InCh_4Cl_2$ octahedra double chains sharing edges and corners with trigonal prismatic units, (b-bottom) common motif build up of cis- and trans edge-sharing octahedra skeins bonded to chains of ethane analogues In_2Ch_6 fragments, (c) coordination of indium species present in the structure.

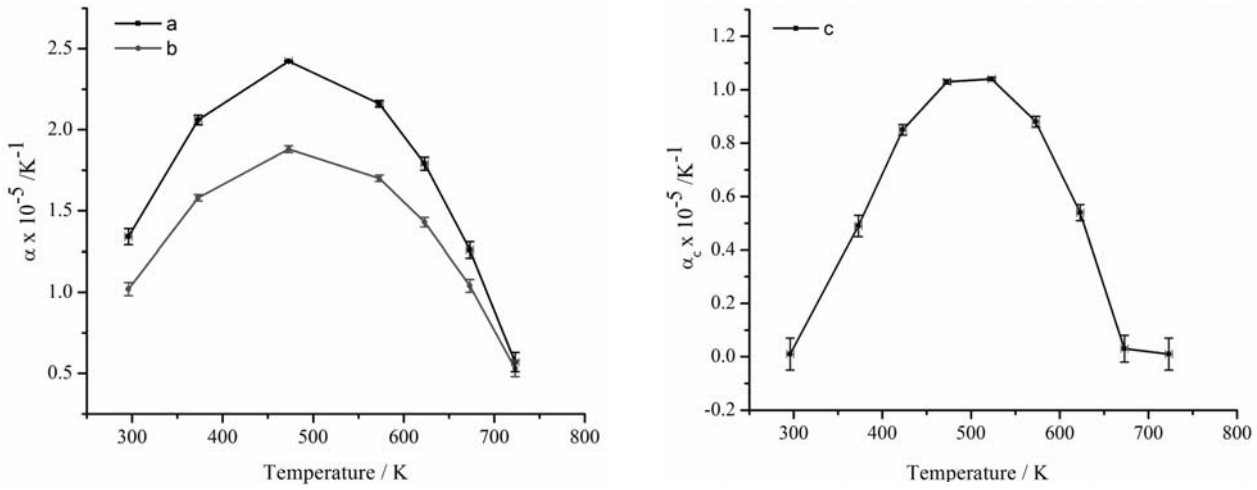

Fig. 4 – The temperature dependence of thermal expansion coefficients along: (a) **a**, **b** directions of In_5S_5Cl and (b) **c** direction for and In_5Se_5Cl.

3. Thermal expansion behavior & coefficients

Based on the thermal behavior of the lattice parameters, it is possible to determine the corresponding expansion coefficients at different temperatures according to the equation (7):

$$\alpha = \frac{1}{L_0}\frac{dL}{dT} \tag{7}$$

where: α represents the thermal expansion coefficient, L_0 is the lattice constant parameter at room temperature (297 K), dL and dT the respective differentials of lattice constants parameters and temperature. The calculation of the standard deviation for each value of the thermal expansion coefficient is done according to the equation (8):

$$\Delta\alpha = \left|\frac{1}{L_0}\cdot\frac{d^2L}{dT^2}\cdot\Delta T\right| \tag{8}$$

where: $\Delta\alpha$ represents the absolute deviation of the expansion coefficient, d^2L/dT^2 the second derivative of the lattice parameters as a functions

of absolute temperature, ΔT is the absolute deviation of the absolute temperature.

The thermal expansion coefficients for In_5S_5Cl and In_5Se_5Cl, are calculated according to the equations (7) and (8) and presented as follows.

Thermal expansion coefficients of **a** and **b** direction for In_5S_5Cl increase with the temperature, reaching the maximal value at 473 K. Right after this temperature a continuous decrease occurs despite the temperature increase (Fig. 4a). A similar increase is observed for the expansion coefficient α_c of In_5Se_5Cl until 473 K (Fig. 4b). After that, a slight increase is observed between the temperature range 473-523 K, after that its values decrease until the difference between consequent values becomes insignificant. The mean thermal expansion coefficients with the respective standard deviations calculated based on equations (6-7) for **a** and **b** directions of In_5S_5Cl are: $\overline{\alpha_a}$ = 1.66(4) x 10^{-5} K^{-1}, $\overline{\alpha_b}$ = 1.31(3) x 10^{-5} K^{-1}, while the linear expansion coefficients for the **c** direction and the unit cell **volume** are: α_c = 1.4(3) x 10^{-5} K^{-1} and α_V = 5.0(5) x 10^{-5} K^{-1} respectively. Based on these results, it can be concluded that the compound In_5S_5Cl reveals comparable expansion coefficients in the three directions. In comparison to the later In_5Se_5Cl displays a higher elongation in **a** and **b** direction compared to **c** direction. Its thermal expansion coefficients in **a** and **b** directions are: α_a = 1.5(3) x 10^{-5} K^{-1}, α_b = 1.2(2) x 10^{-5} K^{-1}, meanwhile the mean coefficients for ***c*** direction and the unit cell volume are $\overline{\alpha_c}$ = 5.4(3) x 10^{-6} K^{-1} and α_V = 3.4(5) x 10^{-5} K^{-1} respectively. A close observation of these data, taking into account their standard deviations, shows a similar elongation of both compounds along [100]. This is slightly higher than the elongation in other directions due to the higher atomic density in this direction which coincides with: a) the direction of edge sharing double octahedra of the characteristic building motif (Fig. 3b-top), and b) the direction of In-In bonds of ethane analogue units coupled to edge sharing double octahedra for the common building motif (Fig. 3b-bottom). Similar expansion behaviour occurs for lattice constant **b** of both compounds. This is in fact the direction of building units stapling or the direction of crystal growth. Unlike the similarities observed in the thermal expansion of **a** and **b** axes of both compounds, their thermal expansion along [001] direction shows discrepancies. The elongation of In_5S_5Cl along [001] is almost 2.6 times higher than the corresponding elongation of In_5Se_5Cl. This discrepancy occurs probably due to the numerous individual crystal anomalies presented by both compounds[1-3] such as: a) polysynthetic twinning, b) lamellar intergrowth and c) crystal intergrowth with similar compounds.

4. Thermal decomposition

At 873 K, diffraction patterns of both compounds (Fig. 1) exhibit merely the presence of In_2S_3 in case of In_5S_5Cl (Fig. 1a), and In_2Se_3 for In_5Se_5Cl (Fig. 1b). According to a detailed investigation the transformation to the end compounds in each case occurs around 723 K. This transformation can be explained by the decomposition mechanism (1):

$$In_5Ch_5Cl \rightarrow 2InCh + In_2Ch_3 + InCl \ (Ch = S, Se) \quad (1)$$

InS, InSe and InCl obtained the during incongruent melting of In_5Ch_5Cl (Ch = S, Se) undergo immediately to phase transitions due to their lower melting points. Meanwhile In_2S_3 (m.p. = 1323 K) and In_2Se_3 (m.p. 933 K) are still crystalline at this temperature range.

The gradual degradation of In_5S_5Cl to InS, In_2S_3 and InCl as a representative of this structure type is exhibited by two fragments of the high-temperature powder diffractions recorded in the temperature range 625 K – 723 K (Fig. 5). The appearing of In_2S_3 reflections at 723 K is arrows pointed.

5. Differential thermal analysis (DTA)

Differential thermal analysis (DTA) were performed in order to endorse the incongruent melting behavior of both ternary compounds, In_5S_5Cl and In_5Se_5Cl. Sections of these measurements are presented in Fig. 6.

The heating curve in case of In_5S_5Cl displays an endothermic effect at approx. 885 K (Fig. 6a) corresponding to its congruent melting. Meanwhile, its cooling curve displays an exothermic effect at 929 K which corresponds to an unusual high solidifying temperature. Post-DTA, X-ray powder diffraction measurements of In_5S_5Cl, displayed mainly the presence of the stable compound In_6S_7 (m.p. 929 K)[4] which contains similar structural conformations as In_5S_5Cl. [1] The binary compound In_6S_7 is obviously obtained as a reaction of solid In_2S_3 and liquid InS according to the reaction (2):

$$In_2S_3 + 4InS \rightarrow In_6S_7 \quad (2)$$

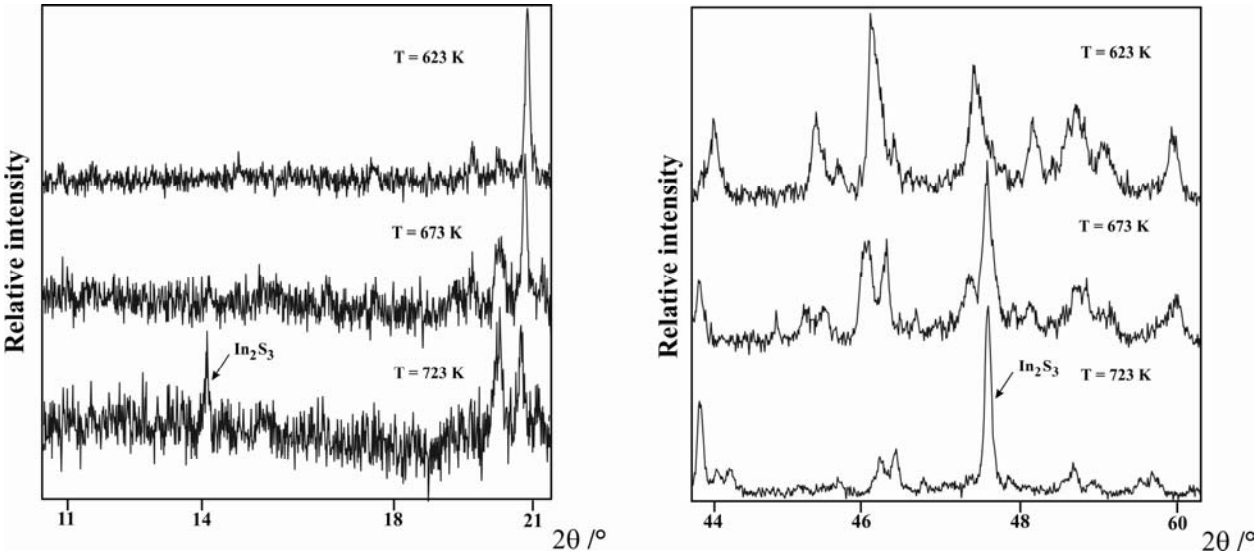

Fig. 5 – Section of the powder diffraction patterns of In_5S_5Cl measured at three different temperatures. An evident sign for the gradual decomposition of In_5S_5Cl is the appearance of the reflection (111) of In_2S_3 between 673 and 723 K.

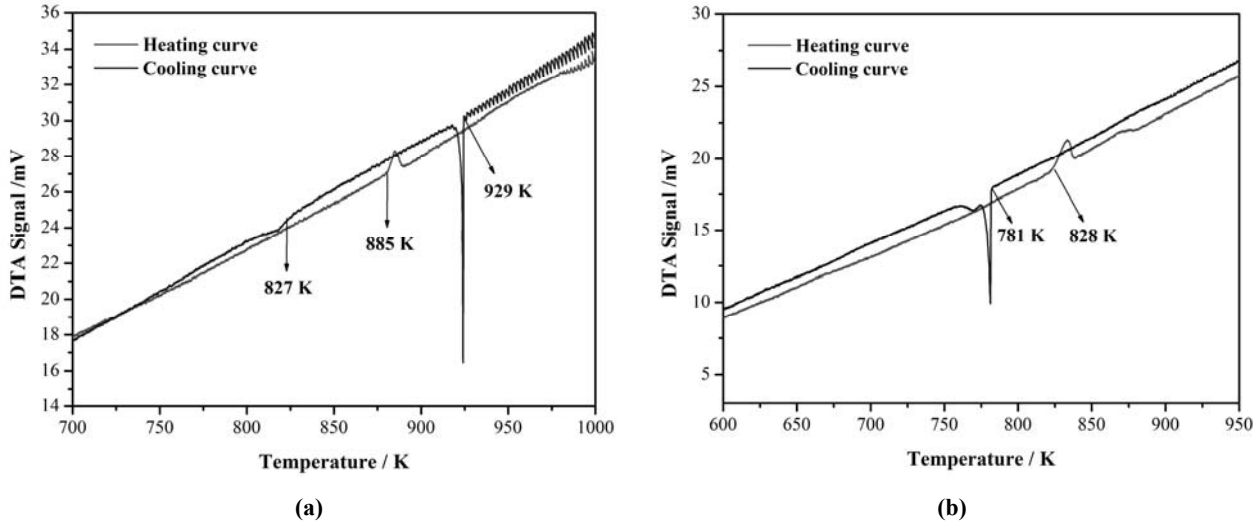

Fig. 6 – Sections of DTA-curves belonging to a) In_5S_5Cl and b) In_5Se_5Cl.

Unlike the sibling compound In_5S_5Cl, In_5Se_5Cl (Fig. 6b), its heating curve displays two endothermal effects. A sharp one at 828 K corresponding to its incongruent melt followed by a broad endothermal effect. These effects are reflected in its cooling curve, where two exothermal effects close to each-other are observable at 781 K and 775 K respectively. Despite it, the XRD powder pattern of the post-DTA sample confirmed merely the presence of In_5Se_5Cl.

EXPERIMENTAL

The needle-shaped single crystals of In_5S_5Cl and In_5Se_5Cl were prepared via solid state methods by annealing at 773 K for two weeks the stoichiometric mixtures of the elements In (tear drop 99.999 %, Chempur, Karlsruhe, Germany), Se (shot 1-3 mm, 99.995 %, Fluka, Buchs, Switzerland) and the binary compound $InCl_3$ (powder, 99.99 %, Heraeus, Hanau, Germany) in evacuated quartz ampoules.[1-2] Bigger crystals were grown by the implementation of a slow temperature program, *i.e.* with low temperature increment (2 K/h). The samples were annealed for two weeks at 773 K and then slowly cooled down with a temperature decreasing rate of 5 K/h until 323 K.

The crystalline compounds In_5S_5Cl and In_5Se_5Cl were ground in an agate mortar in order to obtain small particle sizes ranging from 5-50 μm and transferred into quartz capillaries with the help of a test tube. The choice of capillary diameter depends on the absorption coefficient of the material. For high absorbing materials capillaries of 0.1-0.2 mm outer diameter are used, whereas for medium and low absorbing materials diameters between 0.5 and 1.0 mm are suitable. Extremely high absorbing materials often require a dilution with suitable low absorbing materials such as SiO_2 or BN).

Since the amount of sample and its content strongly depending on the atomic species present often influence the

quality of the diffraction patterns, their indexing and refinement, an alternative simple method is considered to overcome the resulting low reflections intensities and the high background-reflection ratio arising by the high absorption coefficient of these samples. It consisted of the diminishing of the sample volume employed in each measurement using a combination of ∅ 0.1 and 0.2 mm capillaries. In order to obtain such a system, a capillary of ∅ 0.1 mm with a thickness of 0.01 mm was inserted in a ∅ 0.2 mm capillary. The powdered sample was inserted into the free space between both capillaries.

The double capillary system was evacuated and sealed in the presence of H_2-O_2 flame prior of fixing it in the sample holder. The application of this method led to a reduce sample volume inserted in between both capillaries of almost 2/3 of the usual sample volume loaded in 0.1 mm capillary.

The room temperature and high temperature measurements proceeded measuring in region 5-65 ° (2θ), measuring step 0.1° and a ratio time/step 120 sec, ω-rotation = 2.5. The thermal behavior of the selected samples was studied within the interval 296-873 K. For both compounds, the last powder pattern whose reflections could be indexed was recorded at 723 K, at higher temperatures the indexation of the reflections of the diffraction patters led to erroneous determinations.

The high temperature powder diffraction measurements are performed in a STOE Stadi P diffraction system designed for capillary sample holders and/or thin film transmission samples. In each case prior to measurements, the capillary loaded with the powdered crystalline sample was evacuated in order to remove the air in it. The presence of the latter might lead to sample oxidation and/or capillary blast through pressure increase. After that, the capillary was sealed at a length of approx. 2 cm from its top by means of H_2-O_2 flame and fixed on a metallic sample holder using cement as fixing material. The latter was mounted on a goniometer head which allowed the necessary adjustments for reduction of the background intensity.

To average over many crystallites in different positions present in the capillary, a sample rotation of 60 rot/min was employed. On the 2θ arm of the diffractometer a linear PSD (Position Sensitive Detector) was mounted, covering an angular range of Δ2θ = 7-11° depending on the distance between specimen and PSD. The PSD rotation around the sample with respect to the selected 2θ range was controlled externally from the software STOE Stadi P delivered software. The PSD measured in transmission mode covering the 2θ range of 5-90° for room temperature measurements and 5-60° for high temperature measurements. The angular accuracy according the producer ranges 0.001°. For high temperature measurements, the temperature displayed by the control unit could be held constant within about ± 2 K by using a voltage stabilizer. A greater error arises due to the difficulty of measuring the temperature at the position of the sample.

The high temperature attachment consisted of a high temperature ceramic cylinder designed for measurements of quartz capillaries (up to 1300 K) equipped with a U-shaped aperture which allowed the capillary rotation within it and the data collection from PSD in a 2θ range of 5-60°. The thermocouple is mounted closest to the specimen, at the top of the aperture in a position which excludes the interaction with X-ray beam path. The temperature is controlled by an external unit connected to the thermocouple. The whole system is fixed on top of the ω rotating platform of the XRD. The fine capillary adjustment occurred in each case using a portable microscope.

The high temperature equipment attached to STOE Stadi P was calibrated using Iridium as standard since its thermal behaviour has been widely investigated and reported by Schröder *et al*.[13] Prior to measurements, fine crystalline iridium powder with purity 99.9999% delivered by Degussa AG, Germany, was transferred into 0.1 ∅ capillary evacuated and sealed. For the calibration purpose the most intense reflection of Ir 111 was selected and measured within the 2θ range of 35-42° at different setting temperatures with operating parameters: **ω** rotation = 2.5°, scanning step 0.1° and time/step 60 sec. Its exact position in each case was determined latter by the Lorentzian fitting. The lattice constant of Iridium obtained from the 2θ position of the 111 reflection at room temperature (297 K) was 3.8404 Å. Its comparison to the value found for the same temperature by Schröder *et al.* equation[13] 3.8388 Å, reveals a difference of 1.8 x 10^{-3} Å. Accurate temperatures were plotted against the setting temperatures after subtraction of this difference from each obtained lattice constant at the respective temperature found by the equation.

The reflection identification and refinement was performed by the program $WinX^{POW}$ delivered by "STOE" company. The indexation of all peaks was done by Werner's algorithm in case of high symmetry cell and Louer's algorithm in case of low symmetry cell. The indexation started considering the initial 20 peaks and followed by a refinement of all reflections.

Differential Thermal Analysis (DTA) suitable for qualitative investigations of phase transitions and melting behaviours of solids was performed in a "Linseis" device (Type: DTA L-62), Linseis Messgeraete GmbH, Selb, Germany. The sample and the reference (Al_2O_3) were enclosed in preheated evacuated and sealed quartz ampoules of 5 mm outer diameter and 10-20 mm length. The ampoules were placed into ceramic crucibles which were fixed on thermocouples. The samples were heated up to 700°C and cooled down to 50°C using a heating and cooling rate of 5°C/min. The recorded temperature difference between the compound and the reference presented as a peak was evaluated using the delivered Linseis software package. The device calibration was performed using the elements Sn, Zn and Ag in the region of 232-962°C.

CONCLUSIONS

The thermal behaviour of the isotypic mixed valence solids In_5Ch_5Cl (Ch = S, Se) is investigated in this study by means of high-temperature powder X-ray diffraction. A new sample preparation method introducing a combination of ∅ 0.1 mm capillary inserted in a ∅ 0.2 mm capillary is employed in order to overcome the difficulties arising with the X-ray sample adsorption. Despite the numerous structural anomalies bearded by these compounds, their thermal behavior displayed no phase transition within the studied temperature range. The lattice constants **a** and **b** of In_5S_5Cl vary according to a third order polynomial, unlike the lattice constant ***c***

and the unit cell **volume** which exhibit a linear variation. Differently to it, the lattice constants **a, b** and the unit cell **volume** of In_5Se_5Cl vary linearly from temperature; meanwhile, the lattice constant ***c*** obeys to a third order polynomial. In_5S_5Cl reveals comparable expansion coefficients in the three directions. In contrast to it, In_5Se_5Cl displays a higher elongation in **a** and **b** direction compared to ***c*** direction. Unlike the similarities observed in the thermal expansion values of **a** and **b** axes of both compounds, their thermal expansion along [001] direction shows discrepancies. The elongation of In_5S_5Cl along [001] is almost 2.6 times higher than the corresponding elongation of In_5Se_5Cl. Both compounds decompose near 723 K into the respective binary compounds InCh, In_2Ch_3 and InCl (Ch = S, Se). At 873 K only the reflections belonging to the binary solids In_2S_3 and In_2Se_3 are visible due to their high melting temperatures, meanwhile the reflection of the other binary compounds obtained as a consequence of degradation are missing due to their transformation into the amorphous state. The proposed incongruent decomposition of both compounds process is endorsed in each case by parallel DTA measurements.

REFERENCES

1. K. Xhaxhiu, "Insights of Mixed Valence Chalcogenide-Halides of Indium and Thallium", Lambert Academic Publishing, Saarbrücken, 2013, p. 21-95.
2. K. Xhaxhiu, "The use of supercritical carbon dioxide in Solid State Chemistry and basic structural investigations with chalcogenide halides of the third main group", *PhD Thesis*, University of Siegen, 2005, p. 58-130.
3. H.-J. Deiseroth, C. Reiner, K. Xhaxhiu, M. Schlosser and L. Kienle, *Z. Anorg. Allg. Chem.*, **2004**, *630*, 2319-2328.
4. H. J. Deiseroth, H. Pfeifer and A. Stupperich, *Z. Kristallogr.*, 1993, *207*, 45-52.
5. R. Walther, H. J. Deiseroth and *Z. Kristallogr.*, **1995**, *210*, 359.
6. H. J. Deiseroth and C. Reiner, *Z. Anorg. Allg. Chem.*, **1998**, *624*, 1839-1845.
7. R. Walther and H. J. Deiseroth, *Z. Kristallogr.*, **1996**, *211*, 51-52.
8. H. J. Deiseroth and R. Walther, *Z. Kristallogr.*, **1995**, *210*, 88-92.
9. C. Reiner, H. J. Deiseroth, M. Schlosser and L. Kienle, *Z. Anorg. Allg. Chem.*, **2002**, *628*, 1641-1647.
10. C. Reiner and H. J. Deiseroth, *Z. Kristallogr.*, **1999**, *214*, 13.
11. K. Xhaxhiu, C. Kvarnström, P. Damlin, A. Korpa and K. Bente, *J. Eng. & Proc. Manag.*, **2013**, *5*, 81-98.
12. M. B. Robin and P. Day, *Adv. Inorg. Chem. Radiochem.*, **1967**, *10*, 247-422.
13. R. H. Schröder, N. S.-Pranghe and R. Kohlhaas, *Z. Metallkde.*, **1972**, *63*, 12-16.